Genome-wide DNA Methylation Patterns in *Daphnia magna* Reveal Targeting to 5' Exons

Authors

Ruoshui Liu[1], Marco Morselli[2], Lev Y. Yampolsky[3], Leonid Peshkin*[4], Matteo Pellegrini*[1]

[1] Department of Molecular, Cell and Developmental Biology, University of California, Los Angeles, CA 90024, USA

[2] Department of Chemistry, Life Sciences, and Environmental Sustainability, University of Parma, Parma, Italy

[3] Department of Biological Sciences, East Tennessee State University, Johnson City, TN 37614, USA

[4] Systems Biology, Harvard Medical School, Boston, MA 02115, USA

* Corresponding Authors

pesha@hms.harvard.edu

matteop@ucla.edu

ABSTRACT

Daphnia magna is a widely used model organism in ecological and evolutionary studies. DNA methylation in *D. magna* can influence development and adaptation to changing environments. Previous studies have demonstrated that *D. magna* is generally hypomethylated. In this study we characterized the DNA methyltransferases and profiled DNA methylation using whole genome bisulfite sequencing. We find that *D. magna* contains lowly expressed functional methyltransferases and a highly expressed nonfunctional de novo methyltransferase. In line with previous studies, we observe that DNA methylation is found at low levels at CpG dinucleotides, depleted over promoters and elevated in the first exons downstream of the transcription start sites, and that these exons are hypermethylated compared to adjacent introns. In contrast to prior studies in *Daphnia*, we found no significant changes in DNA methylation with age. These observations extend our understanding of the epigenetic landscape in *D. magna*.

KEYWORDS

Daphnia magna; DNA methylation; epigenetic clock; DNA methyltransferase

INTRODUCTION

Daphnia are planktonic crustaceans that live in the freshwater environment. They belong to the Phyllopoda subclass within the class Branchiopoda (1). *Daphnia* are recognized by their flattened leaf-like legs, which generate a water current for their filtering apparatus and are characterized by their uncalcified shell (carapace) (1). Among more than 100 species within the *Daphnia* genus, *Daphnia magna* (*D. magna*) is a widely used model organism in biological research. *D. magna*'s sensitivity and physiological responses to a broad spectrum of drugs, including antibiotics and anti-inflammatory drugs, make it suitable for assessing pharmaceutical toxicity; behavioral ethology studies investigate the vertical migration pattern; and *D. magna* serves as a model organism for studying sexual and parthenogenetic reproduction cycles (2). The utilization of *D. magna* in phenotypic plasticity and ecology further renders it a multifaceted and useful model organism in scientific investigations (2). The estimated genome size of *D. magna* is around 238 mb (BioProject ID: PRJNA624896) (3) and has 2n = 20 chromosomes (4).

In addition to characterizing the genome of *D. magna*, there is also interest in understanding the role of the epigenome. The addition of a methyl group on the 5' carbon of cytosine is carried out by DNA methyltransferases and can influence transcriptional regulation (5). DNA methyltransferases (DNMTs) are a family of enzymes that epigenetically regulate gene expression by establishing and maintaining DNA methylation patterns (6). Humans have 4 DNMTs: DNMT1, DNMT3A, and DNMT3B are canonical, but DNMT3L is inactive. While maintenance methyltransferase DNMT1 is responsible for replicating DNA methylation pattern to daughter cells during cell divisions, functional *de novo* methyltransferase DNMT 3 establishes methyl groups at unmethylated cytosine sites (7,8).

CpG sites in mammals are hypermethylated across the genome (~70% methylation). CpG methylation is associated with gene silencing and is crucial for development (9,10). By contrast, cytosine methylation in *D. magna* is significantly lower with CpG methylation levels around one percent (5). Previous studies have reported that coding exons are hypermethylated relative to other CpGs, and that those of exons 2 to 4 have the highest methylation levels (9,11).

In mammals DNA methylation levels have been established as effective biomarkers for measuring age, and possibly even reflecting the functional capability of organs or organisms (12). DNA methylation-based biomarkers, also known as epigenetic clocks, are identified as one of the most promising estimators of age due to their potential application across all DNA sources and

entire age spectrum (13,14). Epigenetic clocks facilitate understanding the impact of endogenous (epigenetic drift, etc.) and exogenous stress factors and environmental factors on biological aging by comparing an individual's epigenetic age to their chronological age (13,14). In previous studies, an epigenetic clock for *D. magna* was built with 12 clock CpGs (9). However, this analysis was conducted using samples from only two age groups: 10-day and 50-day-old. Additionally, they incorporated *Daphnia* specimens from two different strains and included an interaction term for strain and age in their epigenetic clock. Both the large age gaps and an additional factor of strain potentially diminished the predictive accuracy of their regression model (9). Thus, further research is required to determine the validity of an epigenetic clock for *D. magna*.

The aim of this study was to further characterize DNA methylation patterns in *Daphnia magna*. We first characterized the DNA methyltransferases and measured their expression across life stages. Next, methylation data for five different age groups of *D. magna* were obtained through whole genome bisulfite sequence (WGBS). By aligning the sequence reads to the *D. magna* genome and identifying cytosine methylation sites, we observed a low genome-wide DNA methylation level but distinct methylation patterns across transcripts and exons. Additionally, we analyzed DNA methylation patterns across different ages to investigate age-associated changes.

MATERIALS AND METHODS

Sample collection

A heat-tolerant clone of *D. magna*, IL-MI-8, was originally acquired from the Ebert Lab at the University of Basel, Switzerland. This clone was sourced from a pond in Jerusalem, Israel, as part of Ebert Lab stock collection. To ensure synchronized cohorts, neonates born within a two-day window were separated from their mothers. Sex was determined at 8-9-day old animals. Female individuals were exclusively used in all experiments conducted in this study. All mothers received adequate nutrition and were cultured under identical conditions at 25°C within an incubator. All cultures, including mother cultures, neonate cultures, and tank cultures, were maintained in ADaM water (15). Animals were exposed to a light cycle consisting of 16 hours of light followed by 8 hours of darkness. Animals were fed a daily suspension of the green alga Scenedesmus obliquus at a concentration of 10^5 cells/ml (adjusted for population density, with one animal per 20 ml). Every sixth day, the water was replaced, and offspring were manually

removed until animals were transferred to the culture platform. The operational protocols for the culture platform are akin to those described in previously published protocols (16).

DNA extraction and WGBS library preparation

Approximately 30-50 ng of purified genomic DNA in 50 µl has been subject to sonication using the Bioruptor Pico (Diagenode) for 15 cycles of (30 ON; 90 OFF). Fragmentation patterns have been checked with the D1000HS Assay (Agilent Technologies) on a 4200 TapeStation. The volume of the fragmented DNA has been reduced to 20 µl using a Vacufuge (Eppendorf), then subject to bisulfite conversion using the EZ DNA Methylation-Lightning Kit (Zymo Research). The libraries have been prepared using the Accel-NGS Methyl kit (Swift Biosciences - now xGen Methyl-Seq Library Prep - IDT) according to the manufacturer's recommendations except a major modification. Briefly, the denatured BS-converted cfDNA was subject to the adaptase, extension, and ligation reaction. Following the ligation purification, the DNA underwent primer extension (98C for 1 minute; 70C for 2 minutes; 65C for 5 minutes; 4C hold) using oligos containing random UMI at the location of the i5 barcode. The extension using a UMI-containing primer allows the tagging of each individual molecule in order to be able to remove PCR duplicates and correctly estimate DNA methylation levels. Following exonuclease I treatment and subsequent purification, the libraries were then amplified using a universal custom P5 primer and i7-barcoded P7 primers (initial denaturation: 98C for 30 seconds; 10 cycles of: 98C for 10 seconds, 60C for 30 seconds, 68C for 60 seconds; final extension: 68C for 5 minutes; 4C hold). The resulting single-indexed libraries were then purified, quantified using the Qubit HS-dsDNA assay, the quality checked using the D1000-HS assay (Agilent - TapeStation 4200). The libraries were sequenced as 150 PE on the Illumina NovaSeq6000 platform.

Bisulfite sequencing data processing

Fastq files were aligned to *D. magna* Xinb3 reference genome (BioProject ID: PRJNA624896; D. Ebert, personal communication) using BSBolt Align (default options) (17). PCR duplicates were removed with *samtools markdup* (option -r) v1.15 (18). Alignment number in each sample was counted through *samtools flagstat* (18). The alignment quality of the sequences was evaluated by the CIGAR (compact idiosyncratic gapped alignment report) strings. Sequences with a total sum of matches less than 50 were excluded from further analysis with *samtools view*

and *samtools index*. Alignment index that incorporates a bisulfite-converted sequence for each reference strand was generated using the *BSBolt Index* tool (17). DNA methylation was called using *BSBolt CallMethylation* v1.3.0 (options: -BQ 10 -MQ 20 -IO) with the DNA sequence index as a reference, resulting in CGmap files (17,19).

Data for metagene plots for transcripts, DNA transposons, retrotransposon (SINE), LTR retrotransposon, and non-LTR (LINE) elements with *CGmaptools* (tools: *bed2fragreg*; *mfg*) (19). Data for global DNA methylation level was analyzed with *CGmaptools mstat* for sites with a minimum coverage of 10 (19). *CGmaptools mec* tools were utilized for the average read coverage for cytosines for each chromosome (19).

The matrices of common CGmap sites (with at least 5x coverage) were produced using *BSBolt AggregateMatrix* (17). Only CG sites with a minimum coverage of 5 and present in every sample were included in the CG matrix. UMAP was applied to analyze the similarities between each sample's methylated cytosines (20). The epigenetic clock model was built with the Lasso function from the Python module *sklearn.linear_model* and Leave-One-Out Cross Validation (21).

RNA sequencing

Details of an age-specific RNAseq experiment are reported elsewhere (22). Briefly, RNA was extracted from somatic tissues (whole bodies) of *Daphnia magna* females from laboratory clone GB-EL75-69 (Basel University *Daphnia* Stock Collection, Switzerland) of different ages and reproductive status: young, reproducing (age 15-20 days), old, reproductively senescent, and old, reproductively rejuvenated (age both 130-175 days), in 4 replicates each. In all cases *Daphnia* were sampled within 24 hours of molting and egg-laying and freshly laid eggs (if any) were removed from the brood chamber before homogenizing *Daphnia*. RNAs were extracted using Qiagen RNeasyPlus Mini kit and RNA library preparation performed using NEBNext Ultra II DirecMonal RNA Library prep Kit (NEB, Lynn, MA) following the manufacturer's protocols. The libraries were sequenced with Illumina Novoseq 6000, S4 flow cell, PE100. Reads were mapped to D. magna Xinb3 reference transcriptome (BioProject ID: PRJNA624896; D. Ebert and P. Fields, personal communication) and genes with differential expression either between young vs. old, non-reproducing *Daphnia* or between old reproducing vs. old, non-reproducing ones were identified using DEseq2 (23).

DNA methyltransferase analysis

The functional analysis of DNMT3.1, DNMT3.2, DNMT1, and UHRF1 was conducted using InterProScan (24). Transcript sequences were input into the tool to identify and characterize the functional domains within these methyltransferases.

RESULTS

D. magna has three DNA methyltransferases

Based on the homology with other organisms' DNMTs, *D. magna* harbors two functional and one nonfunctional DNA methyltransferases (**Table S1**) (6). It has two *de novo* DNMTs, *Dma*DNMT3.1 and *Dma*DNMT3.2 (**Figure 1A**) (7). Mammalian DNMT3a/b contains a PWWP domain, an ADD domain, and a methyltransferase (MTase) domain with 6 motifs (I to VI). Non-functional DmaDNMT3.1 is missing 5 critical motifs in the MTase domain, and it is thought to exert similar functions to mammalian DNMT3L. They both contain putatively functional ADD (ATRX-DNMT3A-DNMT3L) domains that do not bind H3K4me3, but the mammalian homologue is missing the PWWP domain (Pro-Trp-Trp-Pro), which has been shown to bind methylated lysines (H3K36me2/3 in mammals) (8). Conversely, the "active" *de novo* DNA methyltransferase, *Dma*DNMT3.2, contains all six DNA methyltransferase motifs and the ADD domain, suggesting that it can sense the methylation status of H3K4 and bind unmethylated H3K4 histones (7). However, it is missing the N-terminal PWWP domain, present in the mammalian active *de novo* DNA methyltransferases (DNMT3A, DNMT3B).

The other putatively active DNA methyltransferase in *D. magna* is *Dma*DNMT1, the maintenance methyltransferase. Compared to the human counterpart, it is missing the N-terminal domains involved in the targeting to the replication foci (DMAP1-BD and PCNA-BD) and a clear nuclear localization signal (NLS). A phosphatase-specific domain (PAP2-wunen) at the N-terminal region is unique to *D. magna* DNMT1.

RNA sequencing data for *D. magna* on three diverse groups - old, non-reproducing; old, reproducing; and young D. magna - revealed low expression of the functional enzymes DNMT1 and DNMT3.2, while DNMT3.1 exhibited the highest expression among the three (**Figure 1B**).

High Coverage *D. magna* Methylomes

To determine the DNA methylation profiles of *Daphnia magna*, we obtained two 45-day-old Xinb3 clone individuals. Whole-genome bisulfite sequencing was performed as described in Methods, and subsequent sequence alignment was carried out (Table S2). The analysis identified around 56.6 million cytosine within the *Daphnia* genome with a minimum coverage of 10 and a modal coverage of 55. The average coverage across contigs is approximately 60, albeit with large variations (**Figure S1A**).

The original genome assembly consisted of 608 contigs, some of which are short. Around 50% of contigs have length shorter than 20 thousand base pairs and 25% of contigs less than 10 thousand base pairs. A small number of short contigs showed pronounced hypermethylation at CpG sites and had highly elevated coverage, suggesting that they are outliers and possible contaminants. To improve the quality of methylome, alignment filtration was implemented, retaining only the sequences corresponding to the top-performing 97 contigs based on genetic recombination map and optical mapping. Post-contig filtration, 38.4 million methylcytosine sites remained. The mean contig length is 1.3 million base pairs and the average coverage of the contigs remained approximately 60 (**Figure S1B**), accompanied by a substantial reduction in variability across contigs, confirming the enhanced reliability of the filtered contigs.

Besides the two deeply sequenced *D. magna* samples (Daphnia_S1 and Daphnia_S2), an additional 16 *D. magna* samples denoted Daphnia_D1 to Daphnia_D16 were bisulfite sequenced across different age groups: young (9 days), mature (22 to 27 days), and old (51 to 58 days). Similar approaches of alignment and filtration were applied to the 16 samples (**Table S1**). Notably, Daphnia_D7 was excluded from subsequent analyses due to a low alignment percentage.

D. magna DNA CpG sites are methylated at low levels

To elucidate the differences between CpN sites, we computed average methylation levels for each contig using the *CGmaptools mstat* function. CpT and CpC sites exhibited an average methylation level of approximately 1.4%, while CpA methylation was slightly lower with 1.1% methylation (**Figure S2**). By contrast, CpG sites displayed higher average methylation levels, around 1.9%, across all contigs.

We further assessed the methylation distribution at each CpX site, and the corresponding fraction of methylation levels was analyzed. We found that the two *Daphnia* samples had

comparable methylation levels. The methylation levels of CpA, CpT, and CpC sites were distributed similarly (**Figure 2A, 2B, & 2D**). Around 40% of the sites had a methylation level below 0.05, while around 55% had no methylation. Approximately 5% of the sites had a methylation level above 0.05 and less than 0.2% above 0.20. By contrast, CpG sites are hypermethylated (**Figure 2C**). Approximately 6% of the CpG sites had a methylation level above 0.05 and around 1% of the sites above 0.20. Specifically, 0.5% of the CpG sites have a methylation level above 0.80.

D. magna DNA CpG sites are hypomethylated upstream of TSS

In addition to examining the overall methylation trends, we analyzed the methylation profiles within specific groups of sequences, including DNA transposon, retrotransposon, LTR retrotransposon, and non-LTR elements (**Figure S3**). Some short interspersed nuclear elements, such as SINE_U, SINE_B2, and SINE_Alu, were methylated upstream or downstream of the sequence. However, most segments were lowly methylated.

We next examined methylation patterns around genes, within the range of 1 kilobase upstream of the transcription start site (TSS) to 1 kilobase downstream of the transcription end site (TES). While CpA, CpT, and CpC sites consistently exhibited a methylation level of approximately 1.5% (**Figure 3A, 3B, 3D**), CpG methylation displayed greater variability at different positions along transcripts (**Figure 3C**). Specifically, CpG methylation levels were lowest a few hundred bases upstream of the TSS (1.5% methylated) and sharply increased downstream of the TSS, peaking at 4.5%. Subsequently, within the transcript, CpG methylation levels gradually decreased, reaching 1.5%, underscoring the dynamic nature of CpG methylation.

D. magna Exon CpG sites are more methylated than neighboring intron regions

To further explore the landscape of genomic methylation, we examined differential methylation patterns between exons and introns. Exons exhibited an average methylation rate of approximately 2.7%, whereas the nearby intron regions were slightly less methylated with average value 2.5% (**Figure 4A**).

We also examine the methylation levels of the different exons in genes. To address the question, we subsetted the genes comprising more than five exons and examined the methylation levels across the first four exons. We find that there is a significant impact of exon positioning on

methylation levels (**Figure 4B**). Exon 1 had a progressively increasing CpG methylation level, while Exon 2 and Exon 3 showed methylation levels peaking at 6-7%. Conversely, exon 4 exhibited a reduction in methylation. The methylation transition from the Exon 1 to Intron 1 and then to the Exon 2 highlights the introns' hypomethylated state relative to exons.

D. magna methylation patterns do not show a significant correlation with age

To investigate the potential changes in methylation levels associated with aging, we conducted analyses on both the global (**Figure 5A**) and transcript-wide (**Figure 5B**) CpG methylation profiles across distinct age cohorts. The methylation levels were comparable across the age groups. By aggregating the CG sites present in all 17 samples and generating a CG matrix, subsequent UMAP visualization revealed no age-related clustering (**Figure 5C**). Furthermore, to find potential age-related CpG sites in D. magna, we trained an epigenetic clock with the CG matrix through Elastic net cross validation regression (**Figure S4**). However, the correlation between predicted and actual ages was not significant, indicating that age-associated CpG sites are not robust enough to build an epigenetic clock. Thus, our findings indicate an absence of significant age-related methylation patterns.

DISCUSSION

In this study, our primary focus was elucidating the genome-wide and transcript-wide methylation patterns in *Daphnia magna* and analyzing the age-associated variations in methylation levels. We employed whole-genome bisulfite sequencing, achieving a high-coverage methylome with an approximate coverage of 60x. Globally, *D. magna* exhibited an average methylation level of 2%. In comparison, mammals such as mice have an average methylation level of around 80% (25). This difference may be due to the absence of a DMAP-1 binding domain and a nuclear localization signal in DNMT1 of *D. magna*. The nuclear localization signal is crucial for transporting DNMT1 back to the nucleus, whereas the DMAP-1 binding domain facilitates interaction with DMAP-1, a co-repressor that aids DNMT1's maintenance activity (26). The absence of these features in *D. magna's* DNMT1 may lead to its limited activity and the correspondingly low levels of DNA methylation observed. Additionally, the low expression levels of DNMT1 and DNMT3.2 may further explain the overall low methylation levels. The high expression of DNMT3.1 in D. magna might be due to possible other functions, not associated with DNA methylation. For example, DNMT3.1 has been shown to regulate growth and reproduction under starvation conditions (7).

In transcribed regions, *D. magna* has methylation level around 3%, similar to its Arthropod relative *Apis mellifera* (25). This low level may be attributed to the absence of a functional PWWP domain in DNMT3.2. Since the PWWP domain binds to H3K36me2 and H3K36me3, markers typically found in transcribed regions, its absence prevents the active DNMT3.2 from recognizing this signal in gene bodies, resulting in reduced methylation (27,28). The hypermethylation of exons compared to introns is not unique to *Daphnia* but also seen in *Apis mellifera*, suggesting a conserved methylation pattern across Arthropoda (25).

The *D. magna* genome is hypomethylated upstream of the TSS and hypermethylated downstream of the TSS, with methylation levels decreasing along the genes. The hypomethylation at the TSS likely results from the activity of DmaDNMT3.2's ADD domain, which selectively binds to unmethylated H3K4 regions (29). As promoters are typically rich in methylated H3K4, DNMT3.2 doesn't bind and thereby prevents DNA methylation (30). This mechanism is supported by a previous study on *D. magna* that documented a high enrichment of H3K4me3 upstream of the actively transcribed *Actin* gene (6). Additionally, H3K4me3 is also found upstream rather than

within the bodies of DNMT1, DNMT3.1, and DNMT3.2 genes, highlighting the crosstalk between histone modification and DNA methylation (6).

There was no significant age association or clustering discovered for the *D. magna* samples. By contrast, the DNA methylation pattern in vertebrates is highly dynamic and changes with age (31). DNA methylation at promoters is often associated with transcriptional inhibition (31,32). As vertebrates age, their DNA methylation marks are erased and reset at different periods of development, in coordination with changes in gene expression pattern. Thus, the largely constant DNA methylation level of *D. magna* across age underlines the possibility DNA methylation is less coupled to developmental changes in gene expression than in vertebrates, possibly due to the different structure of the DNA methyltransferases.

Few epigenetics clocks have been reported for invertebrates. Recently, an epigenetic clock on *Nasonia vitripennis*, the jewel wasp, using 19 age-predictive CpG sites was found to have a Spearman's P of 0.94 for the correlation between predicted and actual age (33). However, the fact that the clock CpG sites were pre-selected for their age association indicates possible overfitting to their samples. Thus, we still lack robust evidence that epigenetic clocks can be generated for invertebrates.

In this study, our primary emphasis was on the *D. magna* Xinb3 clone. The methylation profiles we elucidated may be slightly altered in other *D. magna* strains. Future research should explore the methylation patterns in additional clones to achieve a more comprehensive understanding. Given the limited correlation between DNA methylation and chronological age, our future attention will shift towards the influence of environmental factors, including temperature and water composition, on methylation dynamics.

Acknowledgement

LP was supported by quadraScope Ventures fund and McKenzie Family Charitable Trust.

Disclosure of interest

The authors declare that the research was conducted in the absence of any commercial or financial relationships that could be construed as potential conflicts of interest.

Data availability of statement

Bisulfite-seq data generated in this study has been deposited within the Gene Expression Omnibus (GEO) repository, accession number GSE267859.

REFERENCE

1. Ebert D. Ecology, epidemiology, and evolution of parasitism in Daphnia. National Library of Medicine; 2005.
2. Tkaczyk A, Bownik A, Dudka J, Kowal K, Ślaska B. Daphnia magna model in the toxicity assessment of pharmaceuticals: A review. Sci Total Environ. 2021;763:143038.
3. Routtu J, Hall MD, Albere B, Beisel C, Bergeron RD, Chaturvedi A, et al. An SNP-based second-generation genetic map of Daphnia magna and its application to QTL analysis of phenotypic traits. BMC Genomics. 2014;15:1–15.
4. Beaton MJ, Hebert PD. Variation in chromosome numbers of Duphnia (Crustacea, Cladocera). Hereditas. 1994;120(3):275–9.
5. Vandegehuchte MB, Lemière F, Vanhaecke L, Berghe WV, Janssen CR. Direct and transgenerational impact on Daphnia magna of chemicals with a known effect on DNA methylation. Comp Biochem Physiol Part C Toxicol Pharmacol. 2010;151(3):278–85.
6. Lindeman LC, Thaulow J, Song Y, Kamstra JH, Xie L, Asselman J, et al. Epigenetic, transcriptional and phenotypic responses in two generations of Daphnia magna exposed to the DNA methylation inhibitor 5-azacytidine. Environ Epigenetics. 2019;5(3):dvz016.
7. Nguyen ND, Matsuura T, Kato Y, Watanabe H. DNMT3. 1 controls trade-offs between growth, reproduction, and life span under starved conditions in Daphnia magna. Sci Rep. 2021;11(1):7326.
8. Lyko F. The DNA methyltransferase family: a versatile toolkit for epigenetic regulation. Nat Rev Genet. 2018;19(2):81–92.
9. Hearn J, Plenderleith F, Little TJ. DNA methylation differs extensively between strains of the same geographical origin and changes with age in Daphnia magna. Epigenetics Chromatin. 2021;14:1–14.
10. Smith ZD, Meissner A. DNA methylation: roles in mammalian development. Nat Rev Genet. 2013;14(3):204–20.
11. Chaturvedi A, Li X, Dhandapani V, Marshall H, Kissane S, Cuenca-Cambronero M, et al. The hologenome of Daphnia magna reveals possible DNA methylation and microbiome-mediated evolution of the host genome. Nucleic Acids Res. 2023;51(18):9785–803.
12. Horvath S. DNA methylation age of human tissues and cell types. Genome Biol. 2013;14:1–20.

13. Duan R, Fu Q, Sun Y, Li Q. Epigenetic clock: A promising biomarker and practical tool in aging. Ageing Res Rev. 2022;81:101743.
14. Horvath S, Raj K. DNA methylation-based biomarkers and the epigenetic clock theory of ageing. Nat Rev Genet. 2018;19(6):371–84.
15. Klüttgen B, Dülmer U, Engels M, Ratte H. ADaM, an artificial freshwater for the culture of zooplankton. Water Res. 1994;28(3):743–6.
16. Cho Y, Jonas-Closs RA, Yampolsky LY, Kirschner MW, Peshkin L. Intelligent high-throughput intervention testing platform in Daphnia. Aging Cell. 2022;21(3):e13571.
17. Farrell C, Thompson M, Tosevska A, Oyetunde A, Pellegrini M. BiSulfite Bolt: A bisulfite sequencing analysis platform. Gigascience. 2021;10(5):giab033.
18. Danecek P, Bonfield JK, Liddle J, Marshall J, Ohan V, Pollard MO, et al. Twelve years of SAMtools and BCFtools. Gigascience. 2021;10(2):giab008.
19. Guo W, Zhu P, Pellegrini M, Zhang MQ, Wang X, Ni Z. CGmapTools improves the precision of heterozygous SNV calls and supports allele-specific methylation detection and visualization in bisulfite-sequencing data. Bioinformatics. 2018;34(3):381–7.
20. McInnes L, Healy J, Melville J. Umap: Uniform manifold approximation and projection for dimension reduction. ArXiv Prepr ArXiv180203426. 2018;
21. Pedregosa F, Varoquaux G, Gramfort A, Michel V, Thirion B, Grisel O, et al. Scikit-learn: Machine learning in Python. J Mach Learn Res. 2011;12:2825–30.
22. Dua IY, Pearson AC, Lowman RL, Peshkin L, Yampolsky LY. Post-senescence reproductive rebound in Daphnia associated with reversal of age-related transcriptional changes. bioRxiv. 2024 Jan 1;2024.04.13.589373.
23. Love MI, Huber W, Anders S. Moderated estimation of fold change and dispersion for RNA-seq data with DESeq2. Genome Biol. 2014;15:1–21.
24. Jones P, Binns D, Chang HY, Fraser M, Li W, McAnulla C, et al. InterProScan 5: genome-scale protein function classification. Bioinformatics. 2014;30(9):1236–40.
25. Feng S, Cokus SJ, Zhang X, Chen PY, Bostick M, Goll MG, et al. Conservation and divergence of methylation patterning in plants and animals. Proc Natl Acad Sci. 2010;107(19):8689–94.
26. Lee GE, Kim JH, Taylor M, Muller MT. DNA methyltransferase 1-associated protein (DMAP1) is a co-repressor that stimulates DNA methylation globally and locally at sites of

double strand break repair. J Biol Chem. 2010;285(48):37630–40.

27. Dukatz M, Holzer K, Choudalakis M, Emperle M, Lungu C, Bashtrykov P, et al. H3K36me2/3 binding and DNA binding of the DNA methyltransferase DNMT3A PWWP domain both contribute to its chromatin interaction. J Mol Biol. 2019;431(24):5063–74.
28. Kolasinska-Zwierz P, Down T, Latorre I, Liu T, Liu XS, Ahringer J. Differential chromatin marking of introns and expressed exons by H3K36me3. Nat Genet. 2009;41(3):376–81.
29. Otani J, Nankumo T, Arita K, Inamoto S, Ariyoshi M, Shirakawa M. Structural basis for recognition of H3K4 methylation status by the DNA methyltransferase 3A ATRX–DNMT3–DNMT3L domain. EMBO Rep. 2009;10(11):1235–41.
30. Bernstein BE, Mikkelsen TS, Xie X, Kamal M, Huebert DJ, Cuff J, et al. A bivalent chromatin structure marks key developmental genes in embryonic stem cells. Cell. 2006;125(2):315–26.
31. Meehan RR, Stancheva I. DNA methylation and control of gene expression in vertebrate development. Essays Biochem. 2001;37:59–70.
32. Varriale A. DNA methylation, epigenetics, and evolution in vertebrates: facts and challenges. Int J Evol Biol. 2014;2014.
33. Brink K, Thomas C, Jones A, Chan T, Mallon E. Exploring the ageing methylome in the model insect, Nasonia vitripennis. BMC Genomics. 2024;25(1):305.

A

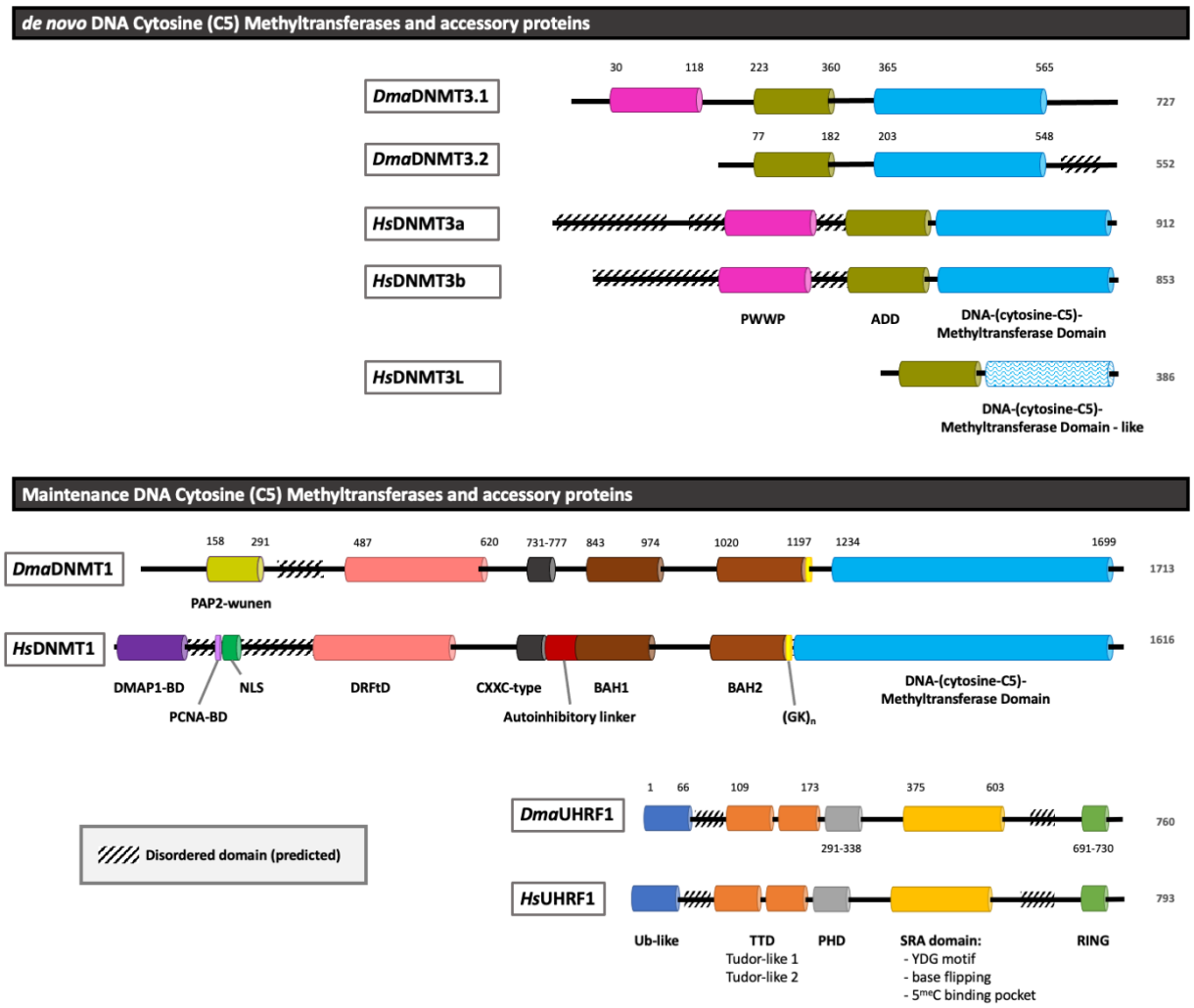

B

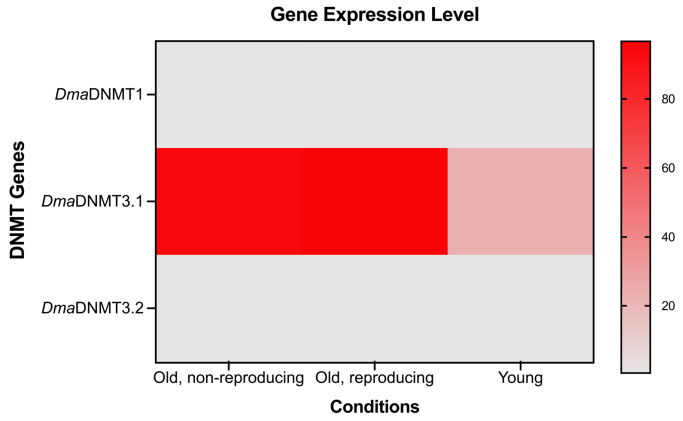

Figure 1. The comparison of DNA (C5) methyltransferases and accessory proteins of *D. magna* and *H. sapiens*. (A) Diagonal black-striped boxes indicate a predicted disordered consensus sequence. Accessory protein domains have been compiled from InterProScan predictions. (B) Gene expression level of 3 DNMT genes under different age conditions.

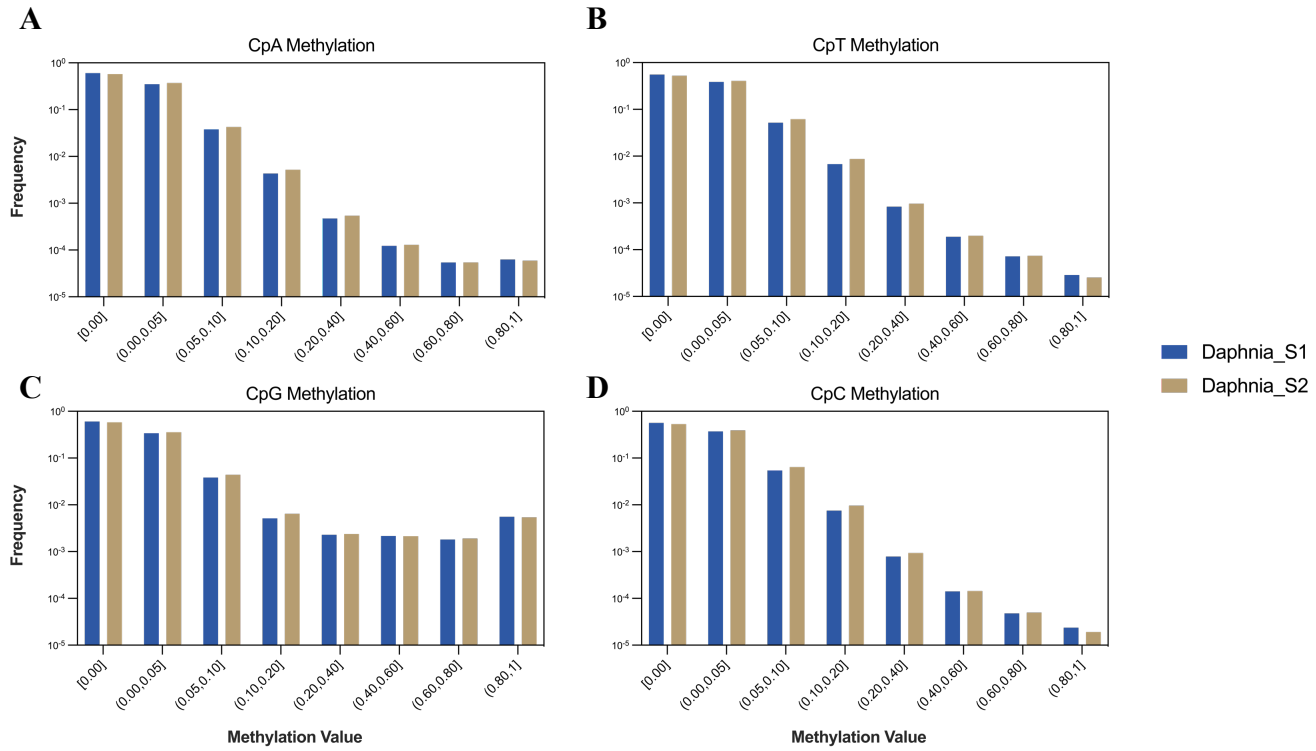

Figure 2. The global DNA methylation level at CpN sites of two deeply sequenced samples. The methylation level quantifies the percentage of methylated sequences at individual sites. The frequency metric indicates the global level of sites with varying methylation levels for (A) CpA, (B) CpT, (C) CpG, and (D) CpC. Notably, CpA, CpT, and CpC sites exhibit comparable distribution patterns, while CpG sites exhibit a higher degree of methylation on average.

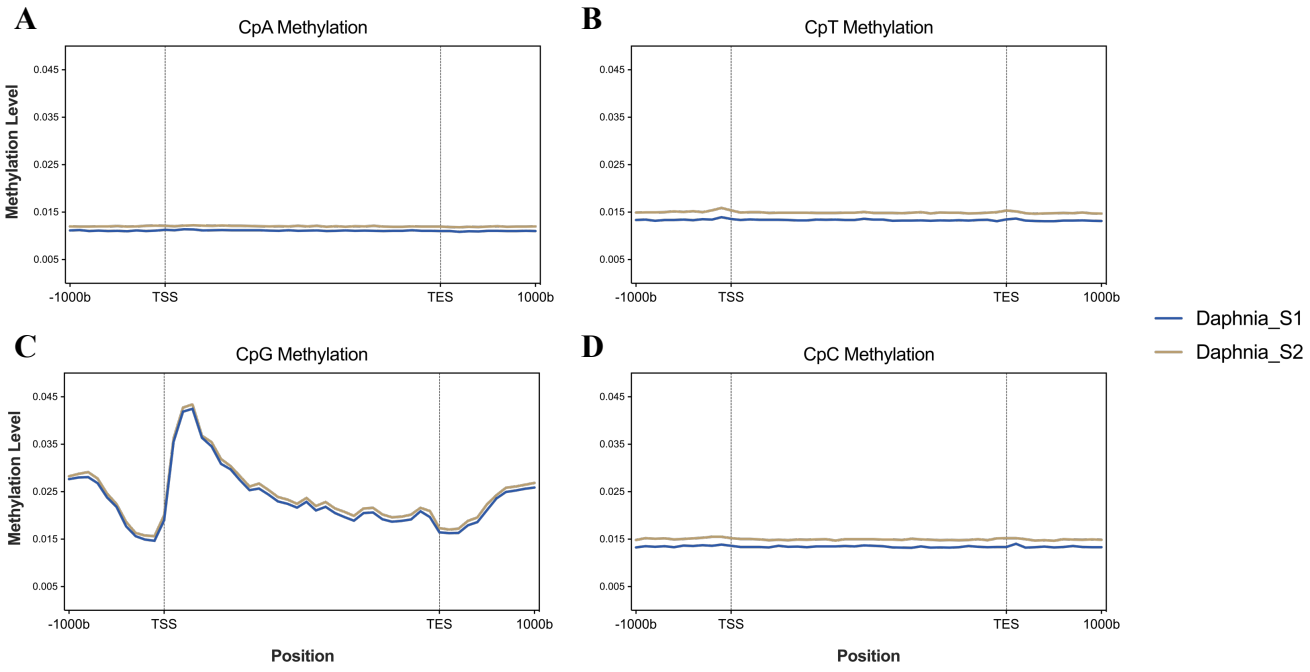

Figure 3. Transcript-wide DNA CpN methylation levels in two deeply sequenced samples, spanning 1 kilobase (kb) upstream and downstream of transcript start and end sites. Each line depicts the average methylation value within a gene for (A) CpA, (B) CpT, (C) CpG, and (D) CpC. CpA, CpT, and CpC sites exhibit uniformly low methylation levels, whereas CpG sites manifest a distinctive pattern. These sites have lower methylation levels at the TSS compared to regions upstream and downstream. TSS: transcription start site; TES: transcription end site.

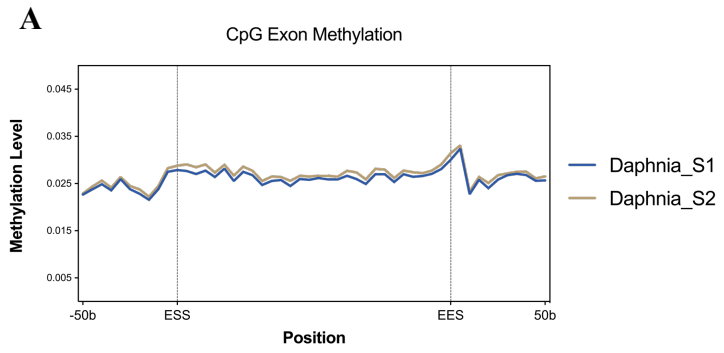

Figure 4. Exon-wide DNA CpG methylation levels in two deeply sequenced samples, spanning 50 bases upstream and downstream of exon start and end sites. (A) Exon CpGs are on average more methylated than adjacent introns. (B) CpG methylation levels of exon 1-4 from genes with more than 5 exons are demonstrated. Exon 2 and Exon 3 are hypermethylated.

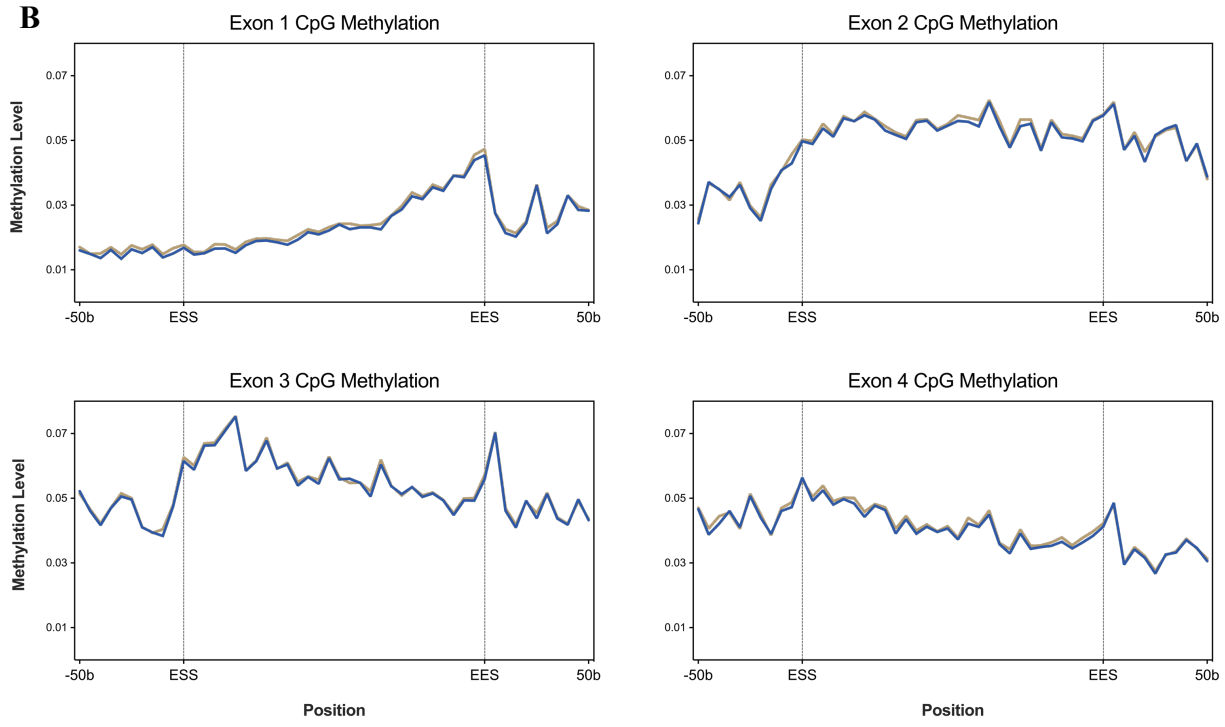

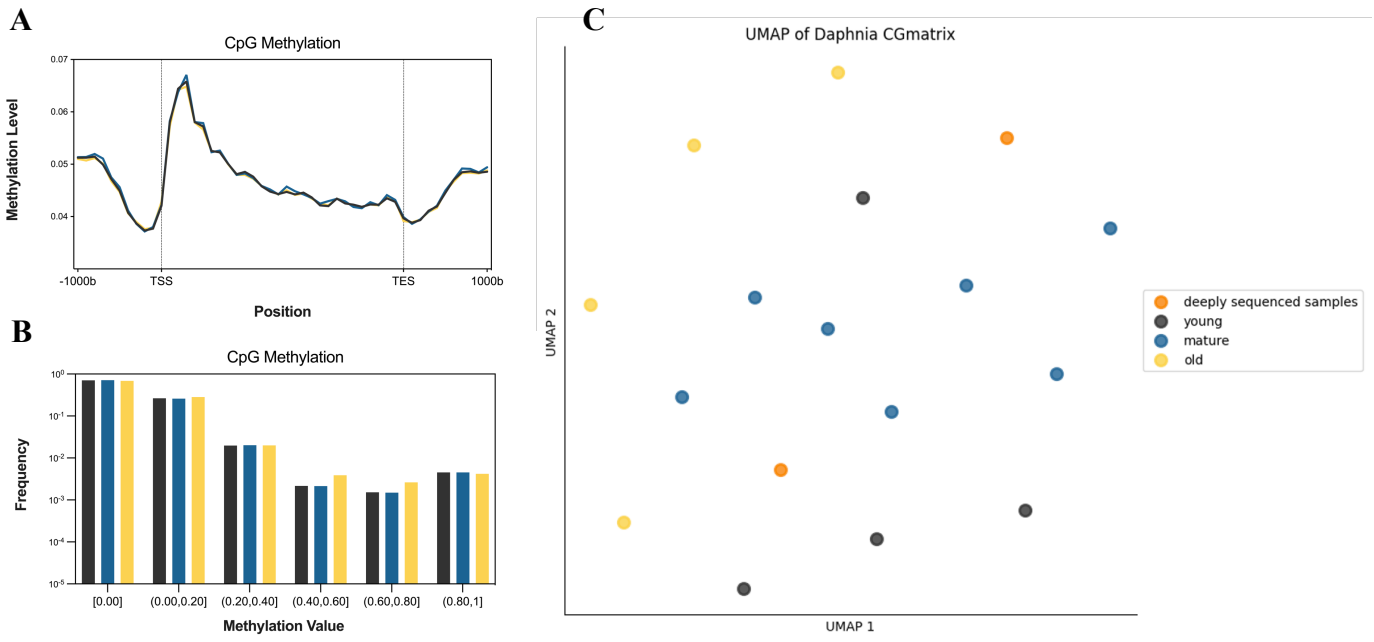

Figure 5. CpN methylation patterns across diverse age groups. (A - B) The global DNA methylation level and transcript-wide DNA methylation level for each age group exhibit similar trends to those observed in the two deeply sequenced samples. There are no significant distinctions in the distributions between the different age groups. (C) The UMAP representation of the *D.magna* consensus methylation matrix does not reveal any age-related patterns.